Advances in Environmental Technology 1 (2018) 23-40

Advances in Environmental Technology

journal homepage: http://aet.irost.ir

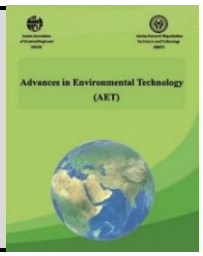

Modeling studies for adsorption of phenol and co-pollutants onto granular activated carbon prepared from olive oil industrial waste

Gehan E. Sharaf El-deen[a,*], Ezzat A. Abdel-Galil[b], Yasser F. El-Aryan[b,c]

[a] *Radioactive Waste Management Department, Hot Laboratories Center, Atomic Energy Authority, Cairo, Egypt*

[b] *Environmental Radioactive Pollution Department, Hot Laboratories Center, Atomic Energy Authority, Cairo, Egypt*

[c] *Chemistry Department, faculty of Sciences, Bisha University, Bisha, Saudi Arabia*

ARTICLE INFO

Article history:
Received 5 June 2017
Received in revised form
25 March 2018
Accepted 25 June 2018

Keywords:
Phenol
Co-pollutants
Isotherm and kinetic models
Activated carbon
Adsorption

ABSTRACT

Granular activated carbon (OSAC) which was derived from olive oil industrial solid waste was chemically activated with different concentrations of phosphoric acid. OSAC-materials were evaluated for their ability to remove phenol from aqueous solution in a batch technique. Adsorption isotherms were determined and modeled with five linear Langmuir forms, namely the Freundlich, Elovich, Temkin, Kiselev and Hill-de Boer models. The experimental data for the adsorption of phenol onto OSAM-materials were fitted well with the Langmuir-1 and 2, Freundlich, Kiselev and Hill-de Boer models. Adsorption was carried out on energetically different sites as localized monolayer adsorption and was an exothermic process. The uptake of phenol onto OSAC increased in the following order: OSAC-80%> OSAC-70%> OSAC-60%; the maximum adsorption capacities of phenol were found to be 114.416, 125.628 and 262.467 mg/g onto OSAC-60%, OSAC-70% and OSAC-80%, respectively. On the other hand, OSAC-80% was used as a good adsorbent for the removal of phenol and Cd^{2+} as co-pollutants from waste aqueous solutions. 80.25% of phenol and 50.66% of Cd^{2+} can be simultaneously removed by OSAC-80%.

1. Introduction

The water pollution resulting from co-contamination with toxic organic pollutants and heavy metals can have detrimental effects on living organisms [1]. Heavy metals and aromatic compounds from industrial activities such as metallurgy, dying and plating are a threat to humans and the environment because of their toxicity and stability after they have been released into the natural environment [2]. Phenol and phenolic compounds are ubiquitous pollutants found in natural water resources created via the effluents of different industrial chemicals from coal refineries, phenol manufacturing, and pharmaceuticals as well as various industries such as resin paint, dying, textile wood, petrochemical, pulp mill, leather, olive oil production, etc. Consequently, aquatic organisms including fish are subjected to these pollutants [3-6]. Phenols, as a class of organics, are similar in structure to the more common herbicides and insecticides in that they are resistant to biodegradation. Phenol is highly soluble in water and very toxic in nature. It is a colorless, hygroscopic and crystalline substance. It is a weak acid dissociating slightly in aqueous solution, and it is known as carbolic acid [7]. In the presence of chlorine in drinking water, phenols form chlorophenol, which has a medicinal taste that is quite pronounced and objectionable [8]. Phenols are considered priority pollutants since they are harmful to organisms at low concentrations. Also, many of them have been classified as hazardous pollutants because of their potential harm to human health [9]. Thus, the removal or annihilation of phenols from waste water is considered a leading environmental problem. The Ministry of Environment and Forests (MOEF), the Egyptian EPA and the USA have listed phenol and phenolic compounds on the priority-pollutants list due to their chronic toxic effects. The MOEF has set the maximum concentration level for industrial effluents at 1mg phenol/l

*Corresponding author. Tel.: +1200301939
E-mail address: gsharaf2000@gmail.com
DOI: 10.22104/AET.2018.2226.1112

for safe discharge into surface water. The WHO recommends the permissible phenolic concentration of 0.001mg/l in potable water [10]. Cadmium is a toxic heavy metal that is commonly present in wastewater. It is highly toxic in any of its chemical forms. The ingestion of cadmium causes muscular cramps, proteinuria, skeletal deformity, nausea, salivation, hypertension, kidney stone formation, Itai disease, chronic pulmonary problems, etc. in humans [11-13]. In addition, Cd (II) ions can replace Zn(II) ions in some enzymes which affects enzyme activity in biological systems. Also, Cd is classified as a human carcinogen by the International Agency for Research on Cancer (IARC) [14]. Several methods have been proposed in the literature for the treatment of phenolic wastewater. These methods include chemical oxidation, precipitation, ion change, solvent extraction, and adsorption [15]. For low volume and high strength phenolic wastewater, granular/powdered activated carbon has been widely used for the adsorption of phenol [16-20]. However, the high cost of activated carbon encourages the examination of cheaper and more feasible raw materials. Sewage sludge, fly ash, coal reject, sawdust, bagasse and fertilizer waste were used as substitute materials for phenol removal [21]. Similarly, several techniques used for the removal of Cd (II) from wastewater include solvent extraction, chemical precipitation, ion exchange, coagulation/flocculation, cementation, electrochemical operations, complexation, biological operations, evaporation, filtration, membrane processes and adsorption [22].

The goals of this work include the following:

(1) To search for a low cost industrial waste as a precursor material for the preparation of activated carbon. Some attempts had been made to produce an efficient OSAC for removing organic pollutants such as phenol and removing co-pollutants as phenol and cadmium ions from aqueous solutions.

(2) To study the applicability of different isotherm models on the experimental data for sorption of phenol onto OSAC that is chemically activated by various concentrations of phosphoric acid. These include the Langmuir, Freundlich, Elovich, Temkin, Kiselev and Hill–de Boer models.

(3) A highly functionalized activated carbon was employed for the removal of co-pollutants, namely heavy metal ions and organic compounds, from aqueous solutions. Phenol was chosen as a model aromatic pollutant with cadmium ions because of its relatively widespread occurrence in wastewater. The main aspects of this study were to examine the effect of temperature, pH and kinetics with the new diffusion kinetic model on the efficient removal of the co-pollutants from aqueous solutions.

2. Materials and methods

2.1. Preparation and characterization of activated carbons

Olive stone solid waste (Os), as a waste product of the olive oil industry, was used as a precursor for the preparation of granular activated carbon samples. First, the raw material was dried and sieved; it had a fraction particle size of about 1 to 2mm. The chemical activation with phosphoric acid as the activating agent was done. Approximately 50g of the obtained Os was weighed three times and impregnated in 200ml phosphoric acid solution at concentrations of 60, 70 and 80 wt%. These mixtures were stirred for 4h at 80-90 ˚C to ensure the arrival of phosphoric acid inside the olive stones. Then, the mixture was filtered and the solids were moved to a tube furnace. Activation of carbon was carried out at a temperature of up to 500 ˚C at a rate of 5 ˚C/min for a hold time of 2h. This step was conducted under an inert N_2-gas with a flow rate of 200ml/min. At the end, the system was left overnight to cool to room temperature with stopping N_2 flow and closing the nozzles of the cylindrical tube of the reactor. The samples were washed with hot distilled water until reaching a pH=6.5, then it was dried at 110 ˚C/ 24h. The oxidized activated carbon samples were designated as OSAC-60%, OSAC-70%, and OSAC-80%.

The characterization of OSAC was determined and has been discussed beforehand in a previous research [23]. The BET-surface area (SBET), the average pore diameter (d) and the bulk densities were found for OSAC-80%, OSAC-70% and OSAC-60% in the following sequence: 1218 m^2/g >779 m2/g >257 m^2/g, 1.1nm>1.0nm>0.954nm and 1g/cm^3>0.84 g/cm^3>0.83 g/cm^3, respectively. This meant that an increase of the phosphoric acid concentration increased the percentage of carbon and porous content. The final OSAC-product had a fraction particle size of about 0.7mm. he FTIR analysis, Figure 1, was discussed in a previous research [23] and showed that the mean peaks were due to: the O–H stretching mode of hydroxyl groups and adsorbed water; the C=O stretching vibrations of ketones, aldehydes, lactones or carboxyl groups; the C–O stretching of acids, alcohols, phenols, ethers and/or esters groups; hydrogen bonded stretching vibration of P=O or P=OOH groups; O-C stretching vibration of P-O-C (aromatic) linkage and –P-O- ionized linkage of acid phosphate esters and/or of symmetrical vibration of P-O-P group [23].

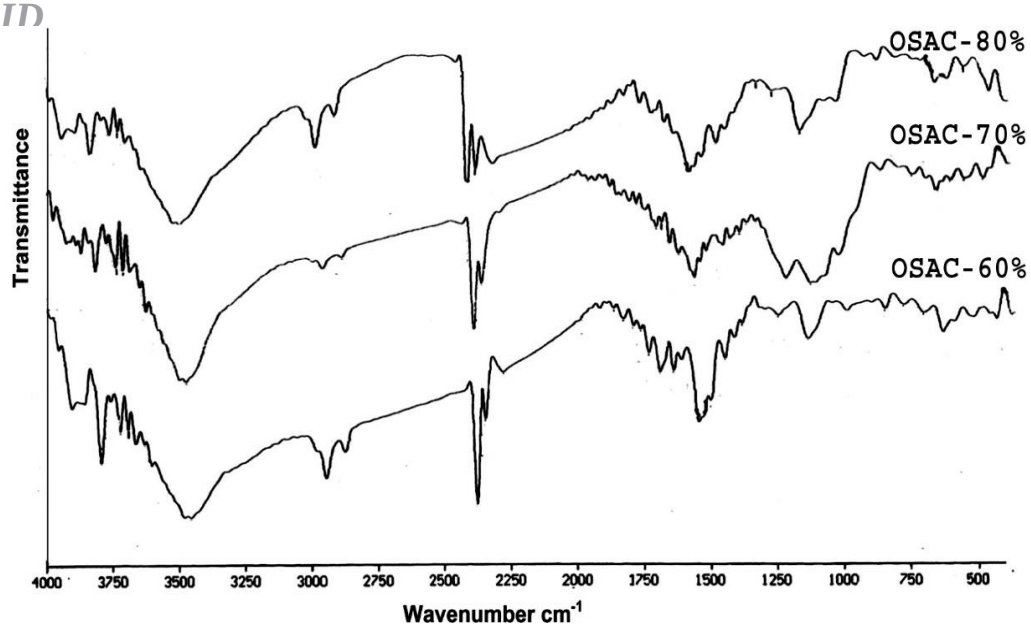

Fig. 1. FTIR spectra of OSAC at different H_3PO_4 acid concentrations

2.2. Materials

All the chemicals employed were of technical grade. Phenol has a freezing point of 39.5-41 ˚C, a molecular weight of 94.11 g/mol. and a solubility of 82 g/l; it was supplied from the El-Nasr Pharmaceutical Chemical Company, Egypt [24]. Cadmium chloride ($CdCl_2$) was purchased from Sigma Aldrich Co., USA. The test solutions containing Cd^{2+} or phenol were prepared by diluting 100 mg/L or 1.0 g/L stock solutions of Cd^{2+} or phenol, respectively, to the desired concentrations. De-ionized water was used for all the experiments. The fresh stock solution of phenol was prepared every day and was stored in a dark brown glass container of 1 L capacity to prevent photo-oxidation.

2.3. Batch adsorption studies

2.3.1. Single organic pollutant

Sorption isotherms studies were conducted using the batch technique by placing a known quantity of the adsorbent (0.6 g/L) in brown glass bottles containing 50 ml aqueous solution of phenol with various concentrations between 50-200 mg/L. The bottles were agitated vigorously in a thermostatic bath. Agitation was continued for 24h., which was higher than the necessary time to reach equilibrium. A stock solution was prepared by dissolving a desired amount of phenol in bi-distilled water without pH adjustment. The testing solutions of the required concentrations were obtained by dilutions. The studies were performed at 25 ˚C. At the end of adsorption process, the adsorbent granules were filtered out and the phenol concentration in the supernatant was then analyzed. The residual concentration of the phenol was determined using double beam UV-visible spectrophotometer (Model: Shimadzu 1601, Japan). The absorbance wavelength of phenol was found at a wavelength of 271 nm. The absorbance calibration curve versus the phenol concentration was exhibited in a linear alternation until 40 mg/L of phenol concentration. Thus, the solutions of phenol concentration higher than 40 mg/L were diluted with bi-distilled water to reach a concentration of less than 40mg/L to ensure an accurate determination of phenol concentration, which lie inside the linear section of the calibration curve.

2.3.2. Co-polluted system (organic and inorganic pollutants)

The batch experiments were carried out to optimize the effect of pH, contact time and temperature on the simultaneous sorption of Cd (II) and phenol by OSAC-80%. The solution pH was adjusted with 0.5 M for both HCl and NaOH for all the experiments. The co-polluted solution was equilibrated for shaking at 12 h at 25±1 ˚C (except for the effect of agitation time at different temperatures studies). Then, the solution was filtered. The filtrate Cd concentration was analyzed using the Atomic Absorption Spectrometer (Hitachi model Z-8100, Germany), and the filtrate phenol concentration was measured using a UV–visible spectrophotometer. The results were plotted by using the percent removal of pollutants.

The sorption uptake (q_t) and the percent Removal (%R) were calculated from the following expressions:

$$q_t = V/m\ (C_o - C_t)\quad \mu g/g \tag{1}$$

$$\%R = [\ C_o - C_e\ )/\ C_o] \times 100 \tag{2}$$

where V is the total volume of salt solution (ml), m is the weight of OSAC used (g), C_o is the initial concentration of the adsorbate (mg/L), C_t is the residual concentration of the

adsorbate (mg/L) at time t, and C_e is the residual concentration of the adsorbate (mg/L) at equilibrium.

3. Theoretical background

3.1. Langmuir model

The Langmuir isotherm [25] is defined as the adsorbent monolayer adsorbed on a definite number of identical sites on the adsorbent surface. The model assumes uniform energies of adsorption onto the surface and no transmigration of adsorbate in the plane of the surface [26]. The Langmuir equation as a nonlinear form can be written as:

$$q_e = \frac{q_{mL} b C_e}{1 + b\, C_e} \quad (3)$$

where q_e is the amount of adsorbate adsorbed per unit weight of adsorbent at equilibrium (mg/g), C_e the equilibrium concentration of the adsorbate in the bulk solution (mg/L), q_{mL} and b are the Langmuir constants related to the maximum adsorption capacity (mg/g) and the rate of adsorption (L/mg), respectively. Eq. (3) can be linearized to five different linear forms as shown in Table 1.

3.2. Freundlich model

The Freundlich isotherm model [27] is an important isotherm used to express the multisite adsorption isotherm for heterogeneous adsorption surface and can be represented by Equation (4).

$$q_e = K_f\, C_e^{1/n} \quad (4)$$

where K_f and n are the Freundlich constants representing the adsorption capacity of the adsorbent ($mg^{\left(1-\frac{1}{n}\right)}\, L^{\frac{1}{n}}\, g^{-1}$) and the intensity of adsorption, respectively.
The Freundlich constants, n and K_f, are determined from the slop and intercept of the linear form of the Freundlich model, as shown in Table 1. The maximum adsorption capacity can be measured according to the Halsey equation [28]:

$$K_f = q_{mF} C_o^{1/n} \quad (5)$$

where C_o is the initial concentration of the solute in the bulk solution (mg/L) and q_{mF} is the Freundlich maximum adsorption capacity (mg/g).

Table 1. Linear forms of Langmuir, Freundlich and Elovich isotherm models

Isotherm model	Nonlinear equation	Linear form	Linear plot
Langmuir-1	$q_e = \frac{q_m b C_e}{1 + b\, C_e}$	$\frac{1}{q_e} = \frac{1}{q_{mL}} + \frac{1}{b q_{mL}} \frac{1}{C_e}$	$\frac{1}{q_e}\ versus\ \frac{1}{C_e}$
Langmuir-2		$\frac{C_e}{q_e} = \frac{1}{q_{mL} b} + \frac{1}{q_{mL}} C_e$	$\frac{C_e}{q_e}\ versus\ C_e$
Langmuir-3		$q_e = q_{mL} - \frac{1}{b} \frac{q_e}{C_e}$	$q_e\ versus\ \frac{q_e}{C_e}$
Langmuir-4		$\frac{q_e}{C_e} = b q_{mL} - b q_e$	$\frac{q_e}{C_e}\ versus\ q_e$
Langmuir-5		$\frac{1}{C_e} = -\, b + b q_{mL} \frac{1}{q_e}$	$\frac{1}{C_e}\ versus\ \frac{1}{q_e}$
Freundlich	$q_e = K_f\, C_e^{1/n}$	$ln\, q_e = ln\, K_f + \frac{1}{n}\, ln\, C_e$	$ln\, q_e\ versus\ ln\, C_e$
Elovich	$\frac{q_e}{q_{mE}} = K_E C_e \exp\left(-\frac{q_e}{q_{mE}}\right)$	$ln \frac{q_e}{C_e} = ln K_E q_{mE} - \frac{q_e}{q_{mE}}$	$ln \frac{q_e}{C_e}\ versus\ q_e$

3.3. Elovich model

The equation defining the Elovich [29] model is based on the kinetic principle assuming that the adsorption sites increase exponentially with adsorption, which implies a multilayer adsorption. It is expressed by the following relation:

$$q_e/q_{mE} = K_E\, C_e \exp\left(-\, q_e/q_{mE}\right) \quad (6)$$

where K_E is the Elovich equilibrium constant (L/mg) and q_{mE} is the Elovich maximum adsorption capacity (mg/g). If the experimental data obeyed the Elovich equation, q_{mE} and K_E-values can be calculated from the slope and intercept of the plot ln (q_e/C_e) versus q_e. The values of q_{mE} and K_E are shown in Table 1.

3.4. Temkin model

The Temkin [30] isotherm can explain the interaction between the adsorbate and the adsorbent active sites according to some assumptions: (i) the heat of adsorption of all the adsorbate molecules in the layer decreases linearly with coverage due to adsorbate-adsorbent interactions; (ii) adsorption is characterized by a uniform distribution of binding energies up to maximum binding energy [31,7].
The Temkin model as a nonlinear form is given by Eq. (7).

$$\theta = {}^{RT}/_{\Delta Q} \ln K_O C_e \quad (7)$$

where ϑ is the fractional coverage, *R* the universal gas constant (kJ mol^{-1} K^{-1}), *T* the temperature (K), ΔQ= (- ΔH) the variation of adsorption energy (kJ/mol), and K_O is the Temkin equilibrium constant (L/mg).

3.5. Kiselev model

The Kiselev equation [32] known as the adsorption isotherm in the localized monomolecular layer and is cleared as a nonlinear form by Eq. (8).

$$k_1 C_e = \frac{\theta}{(1-\theta)(1+K_n\theta)} \quad (8)$$

where *k*1 is the Kiselev equilibrium constant (L mg−1), and K_n is the complex formation constant between adsorbed molecules

3.6. Hill-de Boer model

The Hill-de Boer [33] model describes the case where we have mobile adsorption and lateral interaction among adsorbed molecules and is expressed by the nonlinear regression as:

$$K_1 C_e = \frac{\theta}{1-\theta} \exp\left(\frac{\theta}{1-\theta} - \frac{K_2\theta}{RT}\right) \quad (9)$$

where K_1 is the Hill-de Boer constant (L/mg), ϑ the fractional coverage, *R* is the universal gas constant (kJ/(mol.K), *T* is the temperature (K), and K_2 is the energetic constant of the interaction between adsorbed molecules (kJ/mol.). The positive K_2 means attraction between adsorbates and the negative K_2 value means repulsion between the adsorbed molecules. The apparent affinity for phenol molecules increases with loading when there is an attraction between the adsorbates, and vise-versa. When there is no interaction between the adsorbed molecules (that is K_2 = 0), this Hill-de Boer equation will reduce to the Volmer equation [34].

4. Results and discussion

4.1. Adsorption isotherms

The effect of the initial concentration of phenol adsorbed on different OSAC-materials from aqueous solutions was investigated. Figure 2 shows that the experimental adsorption capacities for phenol onto OSAC-80%, OSAC-70% and OSAC-60% were found to be 97, 92 and 88mg/g, respectively. The theoretical maximum adsorption capacities (q_m theoretical) were calculated using the BET surface area of the studied activated carbons and were found to be 257 m^2/g for OSAC-60%, 779 m^2/g for OSAC-70% and 1218 m^2/g for OSAC-80%; the molecular cross-sectional area of phenol (σ =41.2 A$^{\circ 2}$) [35]. These values are the maximum adsorption capacities, which can be obtained if the molecules are adsorbed flat on the entire adsorbent specific surface [34].

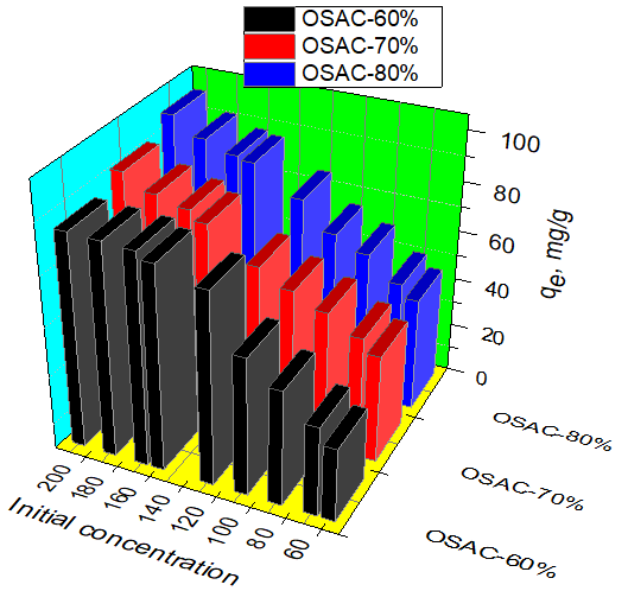

Fig. 2. Effect of initial concentration of phenol adsorbed on different OSAC-materials.

4.2. Models for prediction of sorption isotherm

To evaluate the potential of OSAC-materials on the removal of phenol molecules, different models were suggested to describe the mechanism of adsorption isotherms. Three widely used models were selected for fitting the experimental data as linear form: Langmuir (five linearized expressions), Freundlich and Elovich models. In addition, other models such as the Temkin, Kiselev and Hill-de Boer models in complex equation nature can be solved by non-linear regression fitting. The models were compared against the experimental data to evaluate the best fit. The objective of this work was to select the best isotherm models for predicting the adsorption behavior of phenol molecules onto the OSAC-surface. For this purpose, the residual sum of square of errors (RSSE), root-mean-square error (RMSE) and the correlation coefficients (R^2) associated with the output model results were calculated with the help of the origin 8.5 software program to evaluate the obtained goodness of fit.

4.2.1. Langmuir isotherms

The adsorption data of each adsorbent were resolved by five linearized expressions of the Langmuir-isotherm models. The Langmuir linearized equations are shown in Table 1 and their constants, q_{mL} and b, are summarized in Table 2. Table 2 shows that the maximum monolayer sorption capacity (q_{mL}) values determined by the five Langmuir expressions are higher than that obtained from the experimental data, which are acceptable cases.

Table 2. Parameters of Langmuir, Freundlich and Elovich (applied as linear equations)

Isotherm	OSAC-60 %	OSAC-70 %	OSAC-80 %
Langmuir-1			
b (Lmg^{-1})	0.0286	0.0277	0.0041
q_{mL} ($mg\ g^{-1}$)	101.626	114.155	262.467
RSSE	5.464×10^{-6}	4.281×10^{-6}	9.043×10^{-7}
RMSE	8.835×10^{-4}	6.116×10^{-7}	3.59×10^{-4}
R^2	0.9538	0.9645	0.998
Langmuir-2			
b (Lmg^{-1})	0.021	0.0216	0.0045
q_{mL} ($mg\ g^{-1}$)	114.416	125.628	238.095
RSSE	0.0179	0.0119	0.0068
RMSE	0.0506	0.0412	0.0312
R^2	0.982	0.985	0.9661
Langmuir-3			
b (Lmg^{-1})	0.0263	0.0259	0.0046
q_{mL} ($mg\ g^{-1}$)	105.026	117.358	234.02
RSSE	216.095	240.5	245.74
RMSE	5.556	5.8616	5.92
R^2	0.882	0.901	0.931
Langmuir-4			
b (Lmg^{-1})	0.0236	0.0237	0.00432
q_{mL} ($mg\ g^{-1}$)	109.36	121.531	244.907
RSSE	0.135	0.145	0.0048
RMSE	0.1389	0.148	0.026
R^2	0.882	0.9014	0.931
Langmuir-5			
b (Lmg^{-1})	0.0267	0.0263	0.004
q_{mL} ($mg\ g^{-1}$)	104.264	116.623	265.3
RSSE	4.438×10^{-5}	4.155×10^{-5}	9.698×10^{-7}
RMSE	2.517×10^{-3}	2.436×10^{-3}	3.72×10^{-4}
R^2	0.954	0.964	0.998
Freundlich			
n	2.481	2.395	1.310
K ($mg^{1-1/n}\ L^{1/n}\ g^{-1}$)	11.802	12.345	2.157
q_{mF} ($mg\ g^{-1}$)	88.915	99.58	99.95
RSSE	0.0022	0.0046	0.0132
RMSE	0.0178	0.0256	0.0433
R^2	0.995	0.991	0.988
Elovich			
q_{mE}	43.994	50.35	179.533
K_E	97.833×10^{-3}	91.109×10^{-3}	6.172×10^{-3}
RSSE	0.0386	0.0429	0.012
RMSE	0.0742	0.0781	0.0412
R^2	0.95711	0.96049	0.8993

In order to check the legality of the best Langmuir model for representing the adsorption isotherms of phenol onto the studied activated carbon, two different errors, RSSE and RMSE with R^2 were used. The higher values of R^2 and the lower values of RSSE and RMSA indicated that Langmuir-2 is the best isotherm model for predicting the adsorption behavior of phenol onto OSAC-60% and OSAC-70%. On the other hand, Langmuir-1 is the optimum model for representing the adsorption of phenol onto OSAC-80%. OSAC-materials are good adsorbents in comparison with other materials as shown in Table 3. Therefore, the prepared OSAC-80% was recommended as a good adsorbent for the removal of phenol form aqueous solution.

Table 3. Comparison of adsorption capacities of various activated carbons

Adsorbent	q_{mL} (mg/g)	References
OSAC-60%	114.416	This work
OSAC-70%	125.628	This work
OSAC-80%	262.467	This work
P1	157.7756	[36]
P2	208.3439	[36]
XAD-4	196.4522	[36]
Char500	51.92	[37]
Luffa cylindrica fibers (LC)	9.250694	[38]
Chitin	16.1	[39]
HJ-M05	92.43	[40]
XAD-4	46.04	[40]
XAD-7	36.49	[40]

The essential characteristics of the Langmuir isotherm can be expressed in terms of a dimensionless separation factor (R_L) [42] which is defined by Eq. (10):

$$R_l = \frac{1}{1 + bC_o} \quad (10)$$

where b is the Langmuir constant and C_0 is the highest phenol concentration (mg/L). The value of R_L indicates the type of the isotherm to be either unfavorable ($R_L > 1$), linear ($R_L = 1$), favorable ($0 < R_L < 1$) or irreversible ($R_L = 0$). The values of R_L were found to be 0.326, 0.316 and 0.710 for adsorbents OSAC-60%, OSAC-70% and OSAC-80%. This confirms that the Langmuir isotherm was favorable for the adsorption of phenol onto OSAC under the studied conditions.

4.2.2. Freundlich isotherm

The phenol adsorption isotherm data were analyzed by the Freundlich equation, as linear form, by plotting ln q_e versus ln C_e. The calculated constants of the isotherms, R^2- values and the errors-values are given in Table 2. It was noticed that the linear form of the Freundlich isotherm was more suitable for fitting the experimental data in comparison with the Langmuir forms in case of OSAC-60% and OSAC-70%. This was due to higher R^2-values with lower error-values for the Freundlich isotherm. In contrast, the Langmuir-1 isotherm was more favorable for fitting the experimental data than the Freundlich isotherm in case of OSAC-80%. The magnitude of n-values shows an indication of the adsorption favorability. Where, n-values in the range from 2 to10 represent good, from 1 to 2 moderately difficult, and less than 1 poor adsorption characteristics [43]. Table 2 shows that n-values differ in the range of $2.39 \leq n \leq 26.74$. This indicates that all the studied activated carbons have good efficiency for the adsorption of phenol [43]. In addition, the intensity of the adsorption, n, and the maximum adsorption capacity, q_{mF}, are present in a rising trend with an increasing phosphoric acid concentration activating agent for OSAC.

4.2.3. Elovich isotherm

The adsorption data of phenol onto OSAC-materials were analyzed by a regression analysis of the Elovich model. The Elovich constants, the R^2 and the error-values were calculated by plotting the linear form of the Elovich equation, and they are tabulated in Table 2. It was shown that the lower values of R^2 for all the investigated sorbents indicated that the Elovich model was unsuitable for describing the isotherm experimental data. Suggestions concerning the mechanism of adsorption phenol onto OSAC. To discuss the mechanism of adsorption and the effect of phosphoric acid concentration on the adsorption of phenol, Table 2 shows the effect of the phosphoric acid activating agent on the maximum adsorption capacity of phenol for the Langmuir, Freundlich and Elovich models. The results showed that the impregnation of OSAC in higher concentrations of phosphoric acid produced an increase in the adsorption capacity of phenol in the order 80%OSAC >70%OSAC > 60%OSAC.

The interactions between phenol and activated carbon surface have been explained according to the following possibilities:

1- The diffusion of phenol molecules (phenol molecule diameter is 0.62nm [44]) inside the OSAC pores is possible, where the pore diameters (d) of OSAC-80%, OSAC-70%, OSAC-60% are 1.1nm, 1.0nm and 0.954nm, respectively [23].
2- The π-π dispersion interaction between the π-electrons of the aromatic ring of phenol and those of the aromatic structure of the activated carbon [44].
3- Surface complex formation through electron donor-acceptor interaction, phosphate and carbonyl groups as electron donors and the aromatic rings of phenol as electron acceptor [45]. The strength of donor–acceptor interaction depends mainly on the dipole moment of the oxygen groups on the OSAC plane. The phosphate and carbonyl groups on the activated carbon surface are known as strong donors because of their high dipole moments [46]. Therefore, it is acceptable that the increase in the phosphate groups and basic functional groups on the OSAC

surface shows an essential effect for the adsorption of phenol.

4.2.4. Temkin isotherm

If the adsorption data of phenol on OSAC obeys the Temkin isotherm, the Temkin constant, K_O, and the adsorption energy variation, ΔQ, can be calculated from non-linear regression of the Temkin equation. First, it is important to define the q_m-value, which is used for calculating the surface coverage, θ. It is possible to obtained θ-values from q_m-values. The values of q_m can be obtained from q_{mL} of Langmuir or q_{mF} of the Freundlich models after checking their validity with the experimental results. Also, it is possible to obtain θ-values from the theoretical maximum adsorption capacity. Therefore, the surface coverage, θ, was determined from theoretical, Langmuir and Freundlich maximum adsorption capacities.

The predicted isotherm curves are compared with the corresponding experimental data in Figure 3. It is shown that the experimental results (points) overlapped with the predicted calculated points (lines). All the Temkin parameters as well as the correlation coefficients, RSSE and RMSE, are summarized in Table 4. It was shown that the higher positive values of ΔQ (ΔQ=-ΔH) for all the investigated adsorbents indicated exothermic adsorption for all the adsorbents studied. The positive values of ΔQ decreased with the increasing percentage of phosphoric acid in the order of ΔQ (OSAC-80%) > ΔQ (OSAC-70%) > ΔQ (OSAC-60%) when using theoretical, Langmuir and Freundlich q_m-values. However, the Temkin isotherm model using theoretical-q_m was found to be the best model to represent the experimental data. This is due to higher values of R^2 and lower values of RSSE and RMSE. Therefore, the Temkin isotherm can represent the adsorption isotherm of phenol onto different OSAC samples.

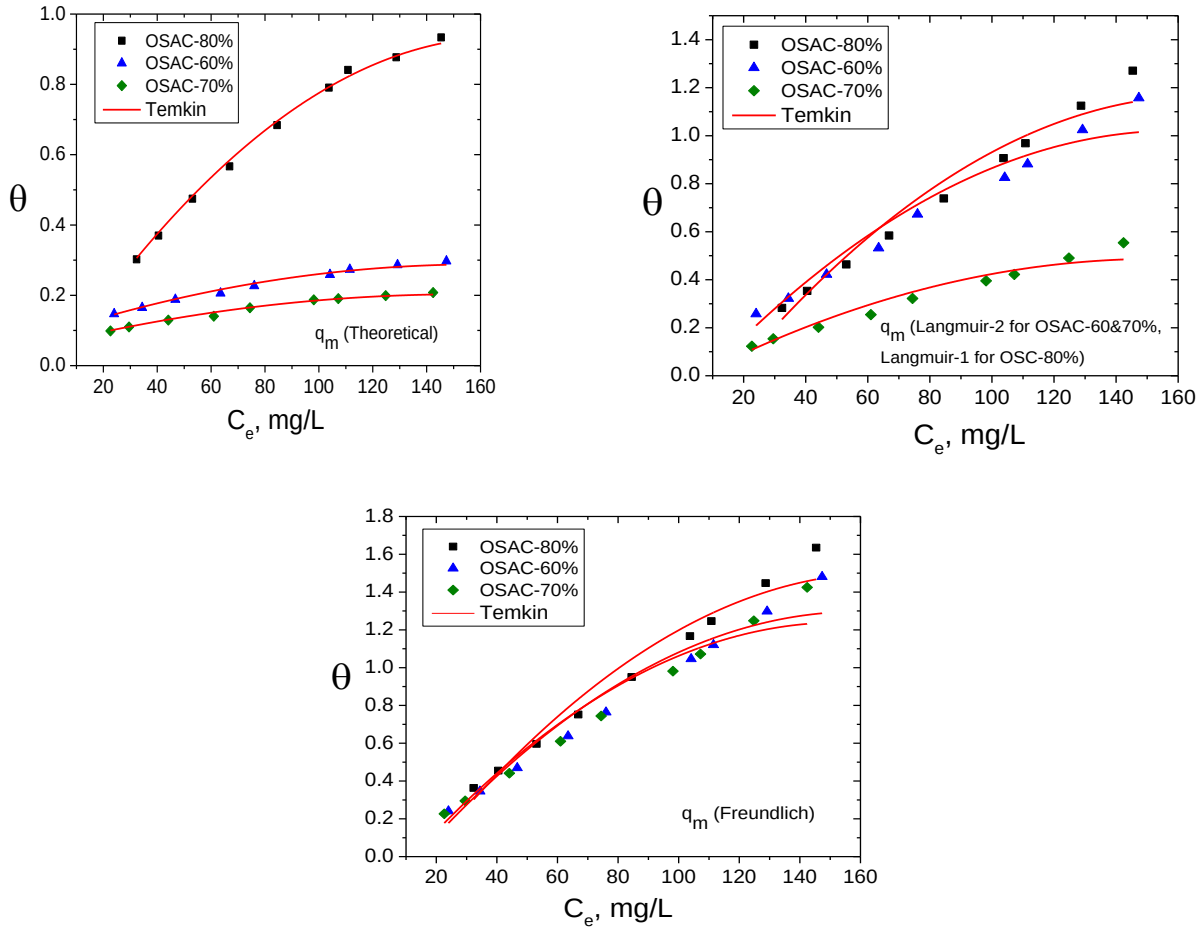

Fig. 3. Comparison of experimental and predicted data of adsorption isotherms of phenol onto OSAC-60%, OSAC-70%, OSAC-80% adsorbents according to Temkin model.

Table 4. Parameters of the Temkin model (as non-linear equations) for the adsorption of phenol onto different adsorbents of OSAC

q_m (mg/g) from:	60 % OSAC	70 % OSAC	80 % OSAC
Theoretical			
K_O (L mg^{-1})	0.19911	0.19679	0.05818
ΔQ (kJmol^{-1})	29164.57205	40785.51427	5766.56959
RSSE	5.088 x 10^{-4}	2.57510^{-4}	0.0026
RMSE	0.0085	0.00606	0.01936
R^2	0.976	0.978	0.993
Langmuir-2 for 60&70% OSAC, and Langmuir-1 for 80% OSAC	0.05643	0.06273	0.04152
K_O (L mg^{-1})	5114.88361	11080.4164	3889.11361
ΔQ (kJmol^{-1})	0.044	0.0104	0.0373
RSSE	0.0793	0.00387	0.0728
RMSE	0.937	0.935	0.956
Freundlich			
K_O (L mg^{-1})	0.04794	0.05148	0.04153
ΔQ (kJmol^{-1})	3712.19866	3953.06721	3023.17904
RSSE	0.084	0.0815	0.0617
RMSE	0.11	0.107	0.0938
R^2	0.937	0.9355	0.956

4.2.5. Kiselev isotherm

The phenol adsorption data were modeled using the non-linear form of the Kiselev isotherm. The simulated isotherm curves are given in Figure 4. The Kiselev constants, namely R^2, RSSE and RMSE, are summarized in Table 5. Table 5 shows that Kiselev fitting is unsuitable for describing the isotherm experimental data in the case of using q_{mL}-data for OSAC-60%, q_{mF}-data for OSAC-80% and q_m-from theoretical data for all studied sorbents. Where, the equilibrium constants of the formation complex between adsorbed molecules, k_n, are negative, which is unexpected because the equilibrium constant should be positive. The negative values of k_n indicate that the complex formation between the adsorbed molecules is not present. Additionally, as noticed from Table 5, in spite of good R^2-values for the Kiselev isotherms of OSAC-70% and OSAC-80% when the surface coverage values were calculated from q_{mL}, the values of RSSE and RMSE are higher. Therefore the Kiselev model can't describe the mechanism of phenol adsorption onto the studied OSAC-samples. This is due to the negative values of K_n and the unacceptable values of k_1, RSSE and RMSE.

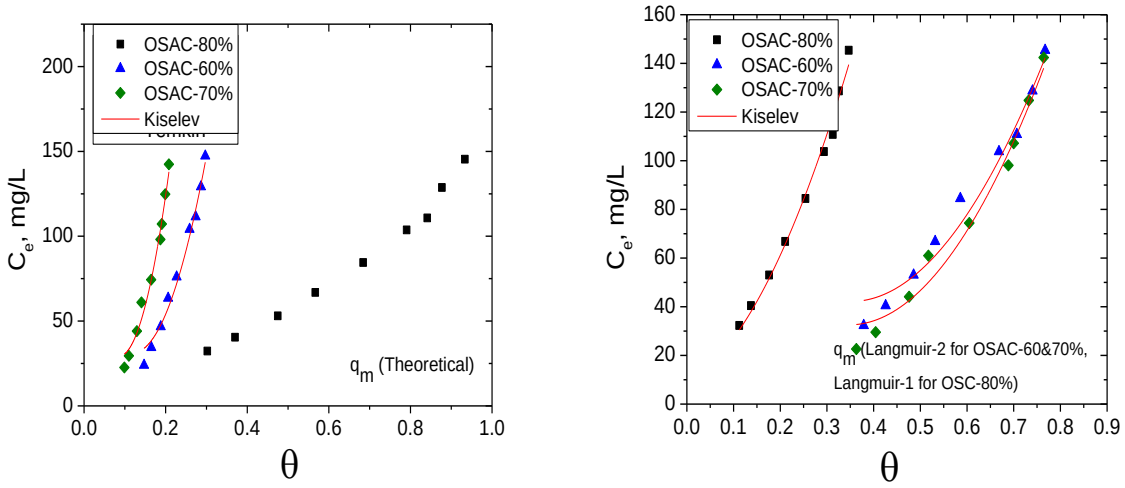

Fig. 4. Comparison of experimental and predicted data of adsorption isotherms of phenol onto OSAC-adsorbents according to Kiselev model

Table 5. Parameters of the Kiselev model (as non-linear equations) for the adsorption of phenol onto different adsorbents of OSAC

q_m (mg/g) from:	60 % OSAC	70 % OSAC	80 % OSAC
Theoretical			
k_1 (L/mg)	-0.00796	0.00583	-0.0207
K_n	-2.1488	-3.28452	-4.777
RSSE	165.141	142.708	8051.997
RMSE	4.857	4.5152	33.916
R^2	0.988	0.99	0.274
Langmuir-2 for 60&70% OSAC, and Langmuir-1 for 80% OSAC	0.0906	0.01721	0.00446
	1.8947	0.39476	-0.43966
k_1 (L/mg)	255.477	169.0418	110.633
K_n	6.0412	4.914	3.975
RSSE	0.977	0.987	0.99128
RMSE			
R^2			
Freundlich			
k_1 (L/mg)	0.0089	-0.0117	-0.00149
K_n	44.455	-11.646	-35.786
RSSE	33117.34	10642.16	8115.55
RMSE	68.78	38.99	34.05
R^2	---	0.1587	0.27

*4.2.6. Hill-de Boer isotherm*In order to examine the agreement of the Hill–de Boer

In order to examine the agreement of the Hill–de Boer model with the experimental results of the adsorption isotherms, the adsorbed amounts at equilibrium are calculated using the equilibrium bulk concentrations and the Hill–de Boer parameters K_1 and K_2, Figure 5. The parameters of the Hill-de Boer isotherm, K_1 and K_2-values as well as R^2, RSSE and RMSE-values are listed in Table 6. Initially, it is important to know that the Hill-de Boer model is applied only when calculating the values of surface covering (θ) from theoretical maximum adsorption capacity. It can be seen in Table 6 that the negative K_2-values decreases with increasing the percentage of the modified phosphoric acid. Thus, the affinity of OSAC samples for phenol adsorption increases in the order of OSAC-80% > OSAC-70% > OSAC-60%. In addition, the good R^2-values indicate that the Hill–de Boer model can describe the experimental isotherms for the adsorption of phenol by the studied adsorbents.

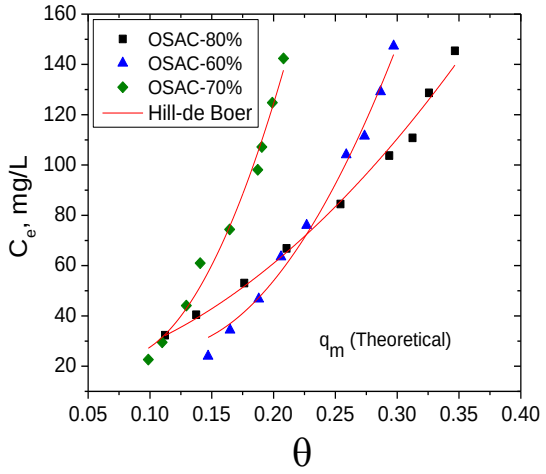

Fig. 5. Comparison of experimental and predicted data of adsorption isotherms of phenol onto OSAC-adsorbents according to Hill-de Boer model

Table 6. Parameters of the Hill-de Boer model

q_m (mg/g) from:	60 % OSAC	70 % OSAC	80 % OSAC
Theoretical			
K_1 (L/mg)	0.01053	0.00869	0.00398
K_2 (kJ/mol)	-153.385	-73.508	-34.314
RSSE	14.543	12.628	7.9154
RMSE	4.557	4.247	3.369
R^2	0.9885	0.99045	0.99287

5. Batch sorption operation for co-pollutant *(phenol\Cd²⁺)* system

5.1. Effect of pH

The effect of pH on the adsorption capacity of OSAC-80% for the removal of 200mg phenol/L and 30mg Cd^{2+}/L at a pH between 2.5 to 11 was investigated, Figure (6:a). The percent removal of phenol slightly increased from a pH of 2.0 to 4.0 and reached approximately 81.7% maximum removal at a pH from 5 to about 10. The molecular form of phenol as a protonated form is the predominant specie at a pH lower than a p*K*a value of 9.89. [47] Therefore, at the acidic medium, phenol adsorption occurs mainly via π-π interaction between the π-electrons of the aromatic ring of the phenol molecules and the π-delocalized electrons on the OSAC-80% structure. In addition, electrostatic attraction was obtained between the negatively charged active groups as electron donors on OSAC-80% surface and the aromatic rings of phenol as the electron acceptor [45]

at the pH from 5 to 9.89, as shown in Figure (6:b). For a pH above the p*K*a value, the phenolate anionic form is the predominant according to ionization of the hydroxyl group in the phenol molecule. Therefore, the adsorption decreases at high pH values due to the electrostatic repulsion force between the adsorbent surface negative charge and the phenolate anions in the solution [48]. In addition, electrostatic repulsion appeared between the adsorbed phenolate anions. A similar trend of pH effect was observed for the adsorption of phenol on activated carbon fibers [49], activated carbon- laboratory grade and commercial grade [50]. On the other hand, for the sorption of Cd^{2+} ions, increasing the initial pH from 2.5 to 11 caused an increase in Cd (II) removal from 10.2% to approximately 99.7%. Moreover, it was noted that the percent removal for Cd (II) ions was lower at a pH less than 4. This may be due to low pH, in which the metal ions suffered a strong repulsive force with the OSAC-80% surface protonated active groups (as P=O, P-O-C and P-O-P groups which noticed from FT-IR spectra) [23], and the percentage of Cd (II) removed was limited. However, a gradual increase in solution pH caused a decrease in H^+ ion concentrations and thus there was an increase in the electrostatic attraction between the cadmium cations (as Cd^{2+} and Cd $(OH)^+$ species) and the negatively-charged active groups on the surface of OSAC-80%. In contrast, at a higher solution pH of more than 8, Cd started to precipitate as $Cd(OH)_2$; therefore, complete removal for Cd-ions at a pH higher than 8 may be corresponding to adsorption and co-precipitation of metal ions onto the adsorbent surface [51,52].

The effect of contact time on the removal of phenol and Cd(II) ions from aqueous solution was studied at 298, 308, 318 and 328K, as shown in Figure 7. The system used 200mg/L and 30mg/L as the initial concentration of phenol and Cd (II), respectively, with an aqueous media of pH 6.0. Figure 7 shows that increasing the temperature caused an acceleration in the sorption rate of the Cd^{2+}-ions and suppression of phenol sorption. The time reached equilibrium at a contact time of 6h for phenol and 3h for Cd^{2+}-ions.

5.3. Adsorption kinetics at different temperatures

In order to investigate the mechanism of adsorption, the kinetic data for the sorption of phenol and Cd^{2+} ions onto the prepared OSAC-80% at different temperatures were analyzed using pseudo first-order, pseudo second-order and diffusion kinetic models.

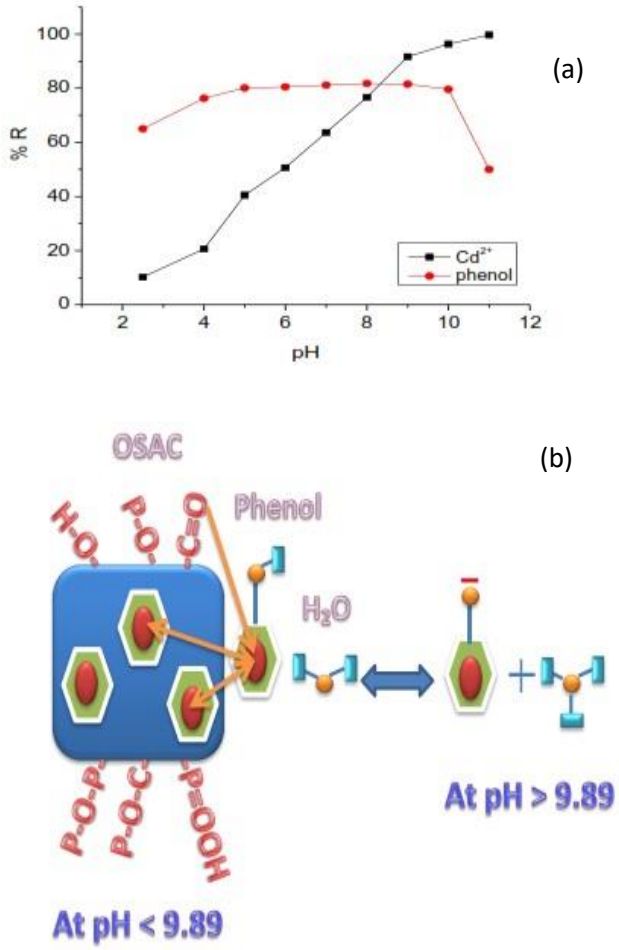

Fig. 6. (a) Effect of pH on co-pollutant (phenol\Cd2+) adsorption onto OSAC-80% (b) and the suggested mechanism of phenol

5.3.1. Pseudo-first-and second order kinetic models

Pseudo-first-order (Eq. (11)) and pseudo-second-order (Eq. (12)) kinetic models [52] were plotted and straight lines were obtained, as shown in Figures 8, 9.

$$\log(q_e - q_t) = \log q_e - \frac{k_1}{2.303} t \quad (11)$$

$$\frac{t}{q_t} = \frac{1}{k_2 q_e^2} + \frac{1}{q_e} t \quad (12)$$

The maximum sorption capacity (q_e (mg/g), rate constants (k_1 (1/min) and k_2 (g/mg min)) and R^2 were calculated and are shown in Table 7.

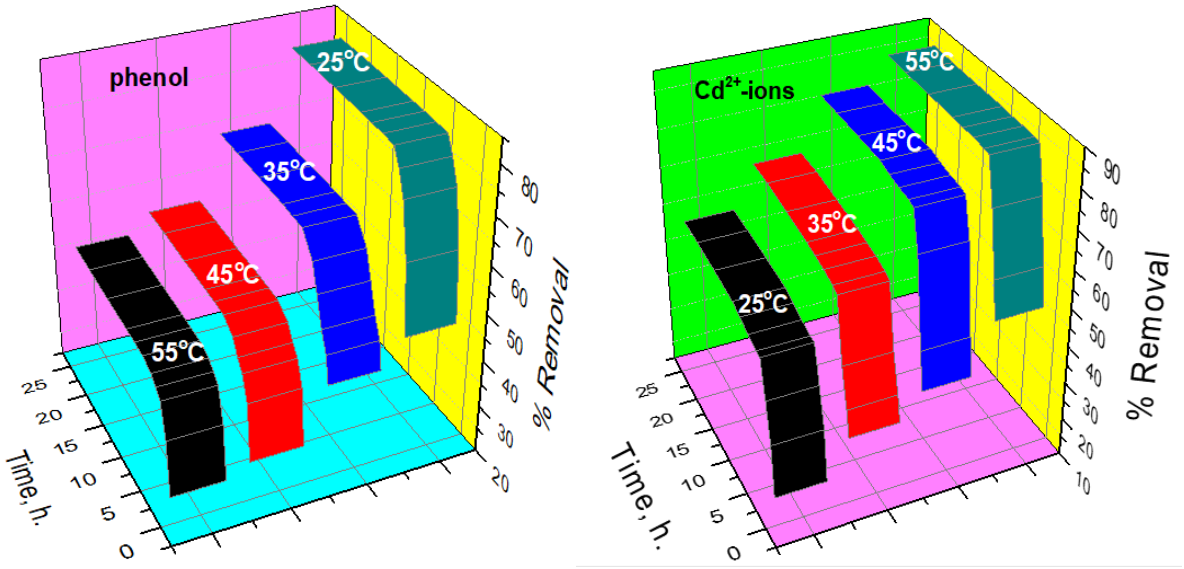

Fig. 7. Effect of time for sorption of co-pollutant onto OSAC-80%

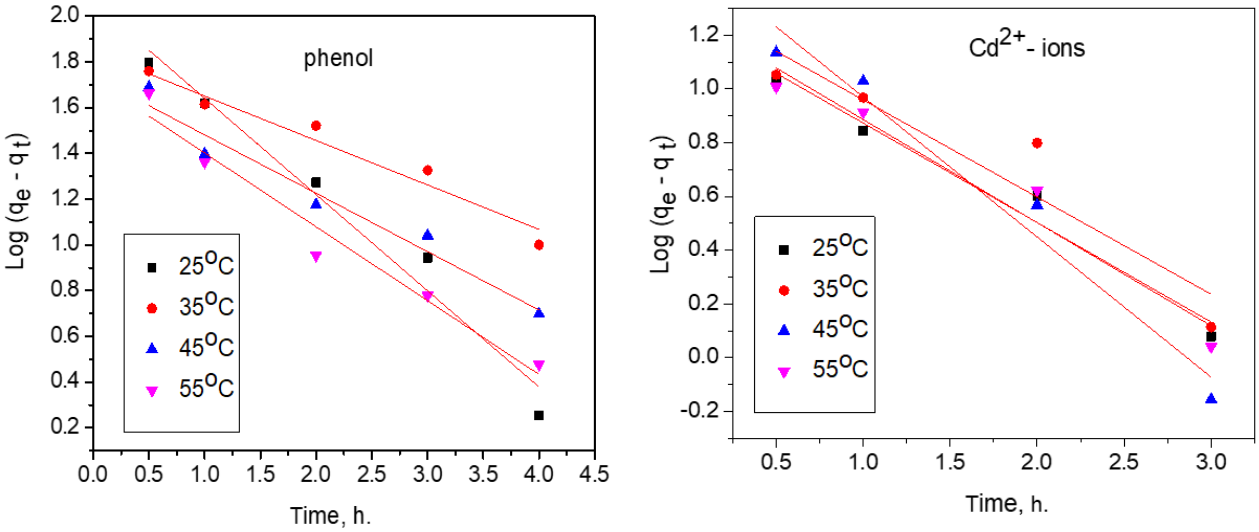

Fig. 8. Pseudo-first order kinetic model for simultaneous sorption of co-pollutant onto OSAC-80%

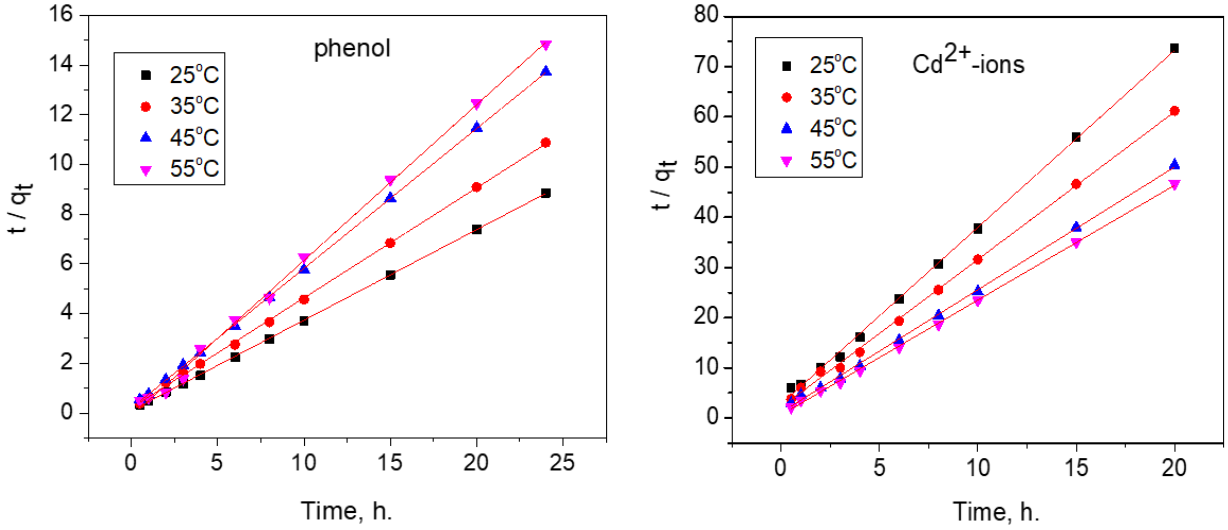

Fig. 9. Pseudo-second order kinetic model for simultaneous sorption of co-pollutant onto OSAC-80%

Table 7. Pseudo-first-order and pseudo-second-order kinetic parameters

Pseudo –first-order kinetic model								
Parameters	**phenol**				**Cd^{2+}- ions**			
	25°C	35°C	45°C	55°C	25°C	35°C	45°C	55°C
q_e^{exp} (mg/g)	161.72	131.62	104.14	96.02	15.5	19	23.7	25.5
q_e^{cal} (mg/g)	125.210	70.039	54.574	53.076	17.07	20.944	30.985	18.616
k_1 (1/min)	0.996	0.447	0.588	0.744	0.852	0.833	1.199	0.883
R^2	0.964	0.939	0.949	0.955	0.960	0.826	0.951	0.931
RSSE	0.0377	0.0147	0.0214	0.0295	0.0138	0.0631	0.033	0.0262
RMSE	0.0126	0.0049	0.0071	0.0098	0.0069	0.0315	0.0167	0.0131
Pseudo –second-order kinetic model								
Parameters	**phenol**				**Cd^{2+}- ions**			
	25°C	35°C	45°C	55°C	25°C	35°C	45°C	55°C
q_e^{exp} (mg/g)	161.72	131.62	104.14	96.02	15.5	19	23.7	25.5
q_e^{cal} (mg/g)	163.13	134.4	105.26	94.97	16.66	19.8	25	27.03
k_2 (g/(mg.min))	$4.66x10^{-4}$	$2.59 x10^{-4}$	$5.10 x10^{-4}$	$5.45 x10^{-4}$	$1.2 x10^{-3}$	$1.25 x10^{-3}$	$1.39 x10^{-3}$	$2.11 x10^{-3}$
R^2	0.999	0.999	0.999	0.999	0.999	0.998	0.998	0.999
RSSE	0.0074	0.0531	0.0167	0.3731	4.667	4.257	2.741	1.171
RMSE	$9.27 x10^{-4}$	$66.4 x10^{-4}$	$21x10^{-4}$	0.0466	0.583	0.5321	0.3427	0.14

As can be seen from Table 7, the experimental data fitted better with the pseudo-second order kinetic model for both solutes. This means that there are strong chemical binding forces between the adsorbate (phenol or Cd^{2+}) and sharing or exchanging electrons on the adsorbent surface [53].It is important to know that the kinetic and equilibrium studies must be complementary, thus adsorption isotherms can be described through kinetic laws. These kinetic laws may be derived from single models. It is possible to establish a kinetic law (diffusion kinetic model) satisfactorily fitting a great numbers of *C* (concentration) vs *t* (time) isotherms. Therefore, the diffusion kinetic model was used to study the adsorption process of phenol and cadmium by OSAC-80%.

5.3.2. Diffusion kinetic model

The diffusion kinetic model is a widely used model to describe the effect of the intra-particle diffusion of solutes on the adsorption rate. In order to assess fitting the experimental kinetic data, the kinetic law of the adsorption process can be described as follows:

$S_S + A_L \leftrightarrow S\text{-}A_S$

This process can be described by the following equation:

$$\frac{-d[A]}{dt} = \frac{-dC}{dt} = k_d . C^{n1} . ((1-\theta)^{n2}) - k_2 . \theta^{n3} \quad (13)$$

where *C* = [A] =concentration of solute (mg/L) in solution at each time t; θ is the coverage surface fraction, which means the solute adsorbed (mg/g)/adsorption capacity of the adsorbent relating to solutes adsorbed in the monolayer (mg/g); k_d is the adsorption rate coefficient; k_2 is the desorption rate coefficient; and *n*1, *n*2, and *n*3 are the partial orders relating to *C*, $(1-\vartheta)$, and ϑ, respectively. Among these parameters, *C* is the only one that may be experimentally determined in a reliable way. θ is the covering surface fraction which may be calculated from *C* as follows:

$$\theta = \frac{C_o - C}{C_o - C_e} \quad (14)$$

where C_o is the initial concentration of solute at time=0 and C_e is the concentration of solute at equilibrium. $n1$-value was determined using the differential method [54,55] based on t=0, θ=0, and (1-θ)=1 at any values of *n*2, and *n*3; Equation (13) can be described as:

$$\left[\frac{-dC}{dt}\right]_o = k_d . C_o^{n1} \quad (15)$$

The best fit has been obtained for *n*2=*n*3=1. For this reason, the kinetic -law corresponding to all the processes studied is:

$$\frac{-dC}{dt} = k_d . C^{n1} . (1-\theta) . k_2 . \theta \quad (16)$$

After the substitution of Eq. [14] in Eq. [16], it follows that:

$$\int_{C_o}^{C} \frac{dC}{(C^{n1} - C_e^{n1}) . (C - C_e)} = \frac{-k_d}{C_o - C_e} . \int_o^t dt \quad (17)$$

After integration of Eq.17 between t = 0 and t (C_0 and C), $n1$=1, it is found that [54]:

$$C = \frac{C_o + k_d . C_e . t}{1 + k_d . t} \quad (18)$$

The plots of the concentration of solutes in solution (C) versus the shaking time (t) for the adsorption of both investigated solutes are shown in Figure (10). The values of C_o, C_e, k_d and R^2 can be calculated from the non-linear fitting of Eq. 18, which are illustrated in Table 8. As shown in Table 8, the higher values of the correlation coefficient (R^2 ≥0.99) and the comparable values of the calculated C_o and C_e to the corresponding experimental values in the case of phenol indicate that the sorption process of phenol follows this diffusion model and its mechanism can be controlled by particle diffusion at all different temperatures studied. In addition, the adsorption rate (k_d) decreases with increasing temperature, indicating that rising temperature can hinder the adsorption of phenol onto OSAC-80%. On the other hand, the adsorption equilibrium of Cd^{2+} at different temperatures is not expressed by this diffusion model according to lower R^2-values and the calculated C_o-values are far from that of the experimental values except at 308K.

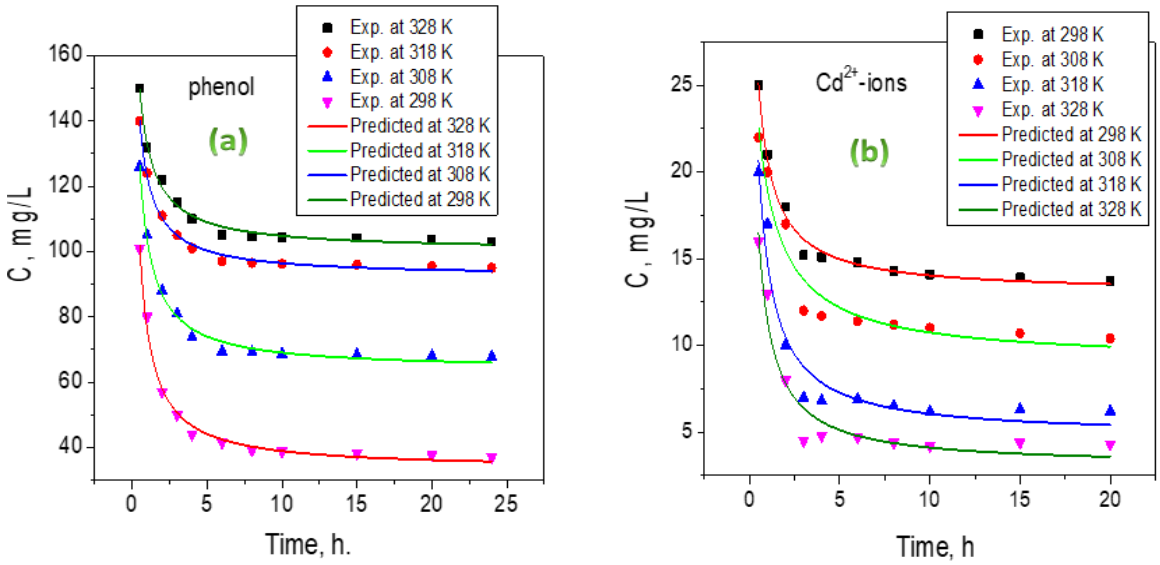

Fig. 10. Diffusion model for sorption of phenol in presence of Cd^{2+} ions (a) and for sorption of Cd^{2+} ions in presence of phenol molecules (b) at different temperatures

Table 8. The calculated initial and equilibrium concentration of solute and the K_d, specific adsorption rate constants at different temperatures

Solute	Temp.,K	C_o , cal.mg/L	C_e , cal.mg/L	C_e , exp.mg/L	K_d,h^{-1}	R^2
	298	202.34746	33.28096	38.70	2.91394	0.99144
Phenol,	308	209.67883	63.70401	68.70	2.64527	0.99041
C_o, exp.	318	201.75951	92.31075	96.00	2.55333	0.99381
=200mg/L	328	202.95335	100.19513	104.15	2.13549	0.99000
	298	41.56218	13.02653	14.42	2.71863	0.98500
Cd^{2+},	308	30.52541	9.05598	11.2	1.17177	0.93002
C_o, exp.	318	43.6644	4.7523	6.55	2.88815	0.93736
=30mg/L	328	37.07513	3.0283	4.47	3.05683	0.93764

The thermodynamic parameters such as free energy change (ΔG^o), enthalpy change (ΔH^o) and entropy change (ΔS^o) were determined using the following equations [56].

$$\Delta G^o = -RT\ lnK_c \quad (19)$$

where K_c is the sorption equilibrium constant, R is the gas constant and T is the absolute temperature (K).

$$\Delta G^o = \Delta H^o - T\ \Delta S^o \quad (20)$$

where ΔH^o and ΔS^o were obtained from the slope and the intercept of the equation (20) by plotting ΔG^o versus T as shown in Figure (11).The values of ΔG^o, ΔH^o and ΔS^o are calculated and given in Table 9. As noticed from Table 9, the negative value of ΔH^o indicates the exothermic nature

for the sorption process of the phenol molecules. This agrees with the results obtained from the isotherm Temkin model, which give higher positive value of the adsorption energy change, ΔQ, where ΔQ=-ΔH. In contrast, the positive value of ΔH^o means endothermic nature of Cd^{2+}-sorption. The entropy change (ΔS^o) was found to be positive for the sorption of phenol, which means increasing the randomness at solid/solution interface during the adsorption process. The opposite was obtained for the sorption of Cd^{2+}-ions onto OSAC-80%. The negative values of ΔG^o indicated the spontaneous nature for adsorption of both solutes. The negativity of ΔG^o values increases with increasing temperature for sorption of Cd^{2+} ions and decreases with increasing temperatures for the sorption of phenol-molecules. This means increasing temperature increases the feasibility for the sorption of Cd^{2+}-ions and inhibit the sorption of phenol onto OSAC-80%.

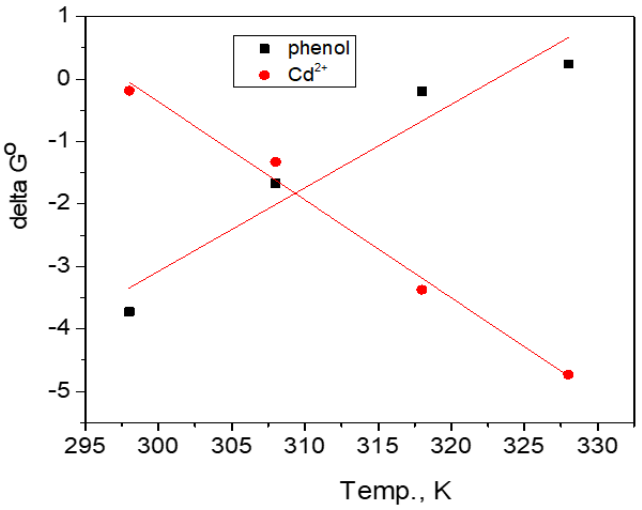

Fig. 11. Gibbs free energy as a relation with temperature for simultaneous sorption of phenol and Cd^{2+}-ions on OSAC-80%

Table 9. Thermodynamic parameters for sorption of co-pollutant onto OSAC-80%

Temp., K	K_c		ΔG°, kJ/mol		ΔH°, kJ/mol		ΔS°, J/mol.K	
	phenol	Cd^{2+}	phenol	Cd^{2+}	phenol	Cd^{2+}	phenol	Cd^{2+}
298	4.195	1.077	-3.724	-0.184				
308	1.919	1.678	-1.670	-1.325	-43.15	46.693	0.134	-0.157
318	1.079	3.580	-0.201	-3.372				
328	0.916	5.666	0.240	-4.730				

6. Conclusions

Olive oil industrial solid waste was used as a cheap precursor to produce olive stone activated carbon that was chemically activated by different H_3PO_4 acid concentrations (OSAC). The Langmuir and Freundlich isotherms models are the best models to describe phenol adsorption onto all the studied OSAC. The monolayer maximum adsorption capacities of phenol onto OSAC-60%, OSAC-70% and OSAC-80% are 114.416, 125.628 and 262.467 mg/g, respectively. Temkin fits well with the equilibrium adsorption data for all the studied adsorbents. The variation of adsorption energy, ΔQ, values decreases with the increasing percentage of the activating agent, phosphoric acid, and higher adsorption is obtained for phenol onto OSAC-80%. In addition, the adsorption of phenol onto the OSAC has an exothermic nature. Hill-de Boer exhibits repulsion between the adsorbed molecules. Therefore, the adsorption of phenol molecules was carried out as localized monolayer adsorption on energetically definite sites on all of the studies OSAC-materials. Furthermore, the functionalized OSAC-80% was conducted to investigate the simultaneous removal of phenol and Cd^{2+} from aqueous solutions using the batch technique. The following conclusion can be drawn from this study: 80.25% of phenol and 50.66% of Cd^{2+} can be simultaneously removed at a pH of 6 by OSAC-80%. The kinetic data for both pollutants reasonably fitted well to the pseudo-second order kinetic model, and the sorption process of phenol can be discussed as particle diffusion according to the good fitting of the diffusion mode. Further, an increase in temperature would cause a rise in the removal of Cd^{2+} and suppress the adsorption of phenol. The sorption process was found to be endothermic for the sorption of Cd^{2+} and of spontaneous nature for both pollutants. OSAC-80% could be a promising adsorbent material for the efficient and effective removal of phenol and Cd (II)-ions from aqueous waste.

Acknowledgments

The work was supported from the Atomic energy authority, Hot laboratories center, Department of Radioactive Waste Management, Cairo, Egypt.

References

[1] Tiwari, D., Lee, S. M. (2016). Surface-functionalized activated sericite for the simultaneous removal of

cadmium and phenol from aqueous solutions: Mechanistic insights. *Chemical engineering journal, 283,* 1414-1423.

[2] Qu, G., Liang, D., Qu D., Huang, Y., Liu, T., Mao, H., Ji, P., Huang, D. (2013). Simultaneous removal of cadmium ions and phenol from water solution by pulsed corona discharge plasma combined with activated carbon, *Chemical engineering journal, 228,* 28-35.

[3] Girodsa, P., Dufoura, A., Fierrob, V., Rogaumea, Y., Rogaumea, C., Zoulaliana, A., Celzardc, A. (2009). Activated carbons prepared from wood particleboard wastes: Characterisation and phenol adsorption capacities, *Journal of hazardous materials, 166* (1), 491-501.

[4] Fleeger, J.W., Carman, K.R., Nisbet, R.M. (2003). Indirect effect of contaminants in aquatic ecosystem. *Science of the total environment, 317*(1-3), 207-233.

[5] Hammam, A.M., Zaki, M.S., Yousef, R.A., Fawzi, O. (2015). Toxicity, Mutagenicity and carcinogenicity of phenols and phenolic compounds on human and living organisms [A Review]. *Advances in environmental biology, 9*(8), 38-48.

[6] Mishra, A. and Poddar, A. (2013). Niyogi Haematology of freshwater Murrel (Channa punctatus Bloch), exposed to Phenolic industrial wastes of the Bhilai Steel plant (Chhattisgarh,India). *International journal of scientific and engineering research, 4*(4), 1866-1883.

[7] Srivastava, V.C., Swamy, M.M., Mall, I.D., Prasad, B., Mishra, I.M. (2006). Adsorptive removal of phenol by bagasse fly ash and activated carbon: Equilibrium, kinetics and thermodynamics. *Colloids and surfaces A: Physicochemical and engineering aspects, 272*(1-2)*,* 89–104.

[8] Rengaraj, S., Seuny-Hyeon, M., Sivabalan, R. Arabindoo, B., Murugesan, V (2002). Agricultural solid waste for the removal of organics: adsorption of phenol from water and wastewater by Palm seed coat activated carbon. *Waste management, 22*(5)*,* 543-548.

[9] Mahvi, A.H., Maleki, A., Eslami, A. (2004). Potential of Rice Husk and Rice Husk Ash for Phenol Removal in Aqueous Systems. *American journal of applied sciences, 1*(4)*,* 321-326.

[10] Yamamura, S. (1963). World health organization, International standards for drinking water, Geneva, Switzerland.

[11] Mahmoud, M.E., Haggag, S.M.S. (2011). Static removal of cadmium from aqueous and nonaqueous matrices by application of layer-by-layer chemical deposition technique. *Chemical engineering journal, 166*(3), 916-922.

[12] Lee, S.M., Lalhmunsiama, L., Tiwari, D. (2014). Sericite in the remediation of Cd (II) - and Mn (II)-contaminated waters: batch and column studies. *Environmental science and pollution research, 21*(5), 3686-3696.

[13] Kula, I., Ugurlu, M., Karaoglu, H., Celik, A. (2008). Adsorption of Cd (II) ions from aqueous solutions using activated carbon prepared from olive stone by $ZnCl_2$ activation. *Bioresource technology, 99*(3), 492-501.

[14] Waisberg, M., Joseph, P., Hale, B., Beyersmann, D. (2003). Molecular and cellular mechanisms of cadmium carcinogenesis. *Toxicology, 192*(2-3)*,* 95-117.

[15] Alves, C.C.O, Franca, A.S., Oliveira, L.S. (2015). Comparison of microwave assisted thermo-chemical procedures in the production of adsorbents for wastewater treatment. *International journal of scientific and development, 6*(12), 888-894.

[16] Zhang, J. (2013). Phenol Removal from Water with Potassium Permanganate Modified Granular Activated carbon. *Journal of environmental protection, 4*(5), 411-417.

[17] Lathasree, S. (2015). Kinetic studies on the removal of phenol in aqueous solutions by adsorption on activated carbon. *Journal of chemical and pharmaceutical research, 7*(3), 1833-1838.

[18] Pirzadeh, K. and Ghoreyshi, A. (2014). Phenol removal from aqueous phase by adsorption on activated carbon prepared from paper mill sludge. *Desalination and water treatment, 52*(34-36), 6505-6518.

[19] Rincón-Silva, N.G., Moreno-Piraján, J.C., Giraldo, L.G. (2015). Thermodynamic Study of Adsorption of Phenol, 4-Chlorophenol, and 4-Nitrophenol on Activated Carbon Obtained from Eucalyptus Seed. *Journal of chemistry, 1*, 1-12.

[20] Jodeh, S., Basalat, N., Abu Obaid, A., Bouknana, D., Hammouti, B., Hadda, T.B., Jodeh, W., Warad, I. (2014). Adsorption of some organic phenolic compounds using activated carbon from cypress products. *Journal of chemical and pharmaceutical research, 6* (2), 713-723.

[21] Rengaraj, S., Seuny-Hyeon, M., Sivabalan, R. (2002). Agricultural solid waste for the removal of organics: adsorption of phenol from water and wastewater by Palm seed coat activated carbon. *Waste management, 22*(5), 543-548.

[22] Purkayastha, D., Mishra, U., Biswas, S., A. (2014). Comprehensive review on Cd (II) removal from aqueous solution. *Journal of water process engineering, 2,* 105-128.

[23] Yakout, S.M., Sharaf El-Deen, G. (2016). Characterization of activated carbon prepared by phosphoric acid activation of olive stones, *Arabian journal of chemistry, 9,* S1155-S1162.

[24] Perry, R.H., Green, D. (1984). Perry's Chemical Engineers' Handbook. 6th ed.; McGraw-Hill.

[25] Langmuir, I. (1916). The constitution and fundamental properties of solids and liquids. *Journal of American chemical society, 38,* 2221-2295.

[26] Hameed, B.H., Rahman, A.A. (2008). Removal of phenol from aqueous solutions by adsorption onto activated

carbon prepared from biomass material. *Journal of hazardous materials, 160* (2-3), 576-581.

[27] Freundlich, H.M.F. (1906). U¨ ber die adsorption in lo¨sungen. *Zeitschrift für physikalische chemie, 57,*385-470.

[28] Halsey, G.D. (1952). The role of surface heterogeneity. *Advances in catalysis, 4*,259-269.

[29] Elovich, S.Y., Larinov, O.G. (1962). Theory of adsorption from solutions of non-electrolytes on solid (I) equation adsorption from solutions and the analysis of its simplest form, (II) verification of the equation of adsorption isotherm from solutions. *Izvestiya akademii Nauk. SSSR, otdelenie khimicheskikh Nauk, 2* (2), 209-216.

[30] Temkin, M.I. (1941). Adsorption equilibrium and the kinetics of processes on nonhomogeneous surfaces and in the interaction between adsorbed molecules. *Russian journal of physical chemistry A, 15,* 296-332.

[31] Srivastava, V.C., Swamy, M.M., Mall, I.D., Prasad, B., Mishra, I.M. (2006). Adsorptive removal of phenol by bagasse fly ash and activated carbon: Equilibrium, kinetics and thermodynamics. *Colloids and Surfaces A: Physicochemical and engineering aspects, 272*(1), 89-104.

[32] Kiselev, A.V. (1958). Vapor adsorption in the formation of adsorbate molecule complexes on the surface. *Kolloid Zhur, 20*,338-348.

[33] Hill, T.L. (1946). Statistical mechanics of multimolecular absorption. ii. Localized and mobile adsorption and adsorption. *Journal of chemical physics, 14*(7), 441-453.

[34] Hamdaouia, O., Naffrechoux, E. (2007). Modeling of adsorption isotherms of phenol and chlorophenols onto granular activated carbon Part I. Two-parameter models and equations allowing determination of thermodynamic parameters. *Journal of hazardous materials, 147*(1-2), 381-394.

[35] Vazquez, G., Gonzalez-Alvarez, J., Garcia, A.I., Freire, M.S., Antorrena, G. (2007). Adsorption of phenol on formaldehyde-pretreated Pinus pinaster bark: equilibrium and kinetics. *Bioresource technology,* 98, 1535-1540.

[36] Păcurariu, C., Mihoc, G., Popa, A., Muntean, S. G. (2013). Ianos R. Adsorption of phenol and p-chlorophenol from aqueous solutions on poly (styrene-co-divinylbenzene) functionalized materials. *Chemical engineering journal*, 222(1), 218-227.

[37] Makrigianni, V., Giannakas, A., Deligiannakis, Y., Konstantinou, I. (2015). Adsorption of phenol and methylene blue from aqueous solutions by pyrolytic tire char: Equilibrium and kinetic studies. *Journal of environmental chemical engineering, 3*(1),574-582.

[38] Abdelwahab, O. and Amin, N.K. (2013). Adsorption of phenol from aqueous solutions by Luffa cylindrica fibers: Kinetics, isotherm and thermodynamic studies. *Egyptian journal of aquatic research, 39* (4), 215-223.

[39] Pigattoa, G., Lodia, A., Finocchioa, E., Palmab, M.S.A. (2013). Chitin as biosorbent for phenol removal from aqueous solution: Equilibrium, kinetic and thermodynamic studies. *Chemical engineering and processing, 70* (1), 131-139.

[40] Huang, J., Zha, H., Jin, X., Deng, S. (2012). Efficient adsorptive removal of phenol by a diethylenetriamine-modified hypercrosslinked styrene–divinylbenzene (PS) resin from aqueous solution. *Chemical engineering journal, 195–196* (1), 40-48.

[41] Carvajal-Bernal, A.M., Gómez, F., Giraldo, L., Moreno-Piraján, J.C. (2015). Adsorption of phenol and 2, 4-dinitrophenol on Activated Carbons with Surface Modifications. *Microporous and mesoporous materials, 209*, 150-156.

[42] Hall, K.R., Eagleton, L.C., Acrivos, A., Vermeulen, T. (1966). Pore-and solid-diffusion kinetics in fixed-bed adsorption under constant-pattern conditions. *Industrial and engineering chemistry fundamentals, 5* (2), 212–223.

[43] Treybal, R.E. (1981). Mass-transfer Operations, 3rd Ed, McGraw-Hill.

[44] Valente Nabaisa, J.M., Gomesa, J.A., Suhasa, Carrott, P.J.M., Laginhasa,C., Romanb, S. (2009). Phenol removal onto novel activated carbons made from lignocellulosic precursors: Influence of surface properties. *Journal of hazardous materials, 167*(1-3)*,* 904-910.

[45] Dabrowski, A., Podkoscielny, P., Hubicki, Z., Barczak, M. (2005). Adsorption of phenolic compounds by activated carbon, a critical review. *Chemosphere, 58*(8), 1049-1070.

[46] Vereshchagina, Y.A., Chachkov, D.V., Alimova, A.Z., Malysheva, S.F., Gusarova, N.K., Ishmaeva, E.A., Trofimov, B.A. (2014). Dipole moments and conformational analysis of tris (2-pyridyl) phosphine and tris (2-pyridyl) phosphine chalcogenides: Experimental and theoretical study. *Journal of molecular structure, 1076*, 285-290.

[47] Thinakaran, N., Baskaralingam, P., Pulikesi, M., Panneerselvam, P., Sivanesan, S. (2008). Removal of Acid Violet 17 from aqueous solutions by adsorption onto activated carbon prepared from sunflower seed hull. *Journal of hazardous materials, 151,* 316-322.

[48] Hameed, B.H., Rahman, A.A. (2008). Removal of phenol from aqueous solutions by adsorption onto activated carbon prepared from biomass material. *Journal of hazardous materials, 160*(2-3)*,* 576-581.

[49] Liu, Q., Zheng, T., Wang, P., Jiang, J., Li, N. (2010). Adsorption isotherm, kinetic and mechanism studies of some substituted phenols on activated carbon fibers. *Chemical engineering journal, 157*(2-3), 348-356.

[50] Srivastava, V.C., Swamy, M.M., Mall, I.D., Prasad, B., Mishra, I.M. (2006). Adsorptive removal of phenol by bagasse fly ash and activated carbon: equilibrium, kinetics and thermodynamics. *Colloids and surfaces A: Physicochemical and engineering aspects, 272*(1-2), 89-104.

[51] Lee, S.M., Lalhmunsiama, Tiwari, D. (2014). Sericite in the remediation of Cd (II) - and Mn (II)-contaminated waters: batch and column studies. *Environmental science and pollution research*, *21*(5), 3686-3696.

[52] Lalhmunsiama, Tiwari, D., Seung-Mok Lee, S-M. (2016). Surface-functionalized activated sericite for the simultaneous removal of cadmium and phenol from aqueous solutions: Mechanistic insights. *Chemical engineering journal,* 283, 1414-1423.

[53] Foo, K.Y., Hameed, B.H. (2010). Insights into the modeling of adsorption isotherm systems. *Chemical engineering journal,* 156(1), 2-10.

[54] Valenzuela-Calahorro, C., Cuerda-Correa, E., Navarrete-Guijosa, A., Gonzalez Pradas, E. (2002). Application of a Single Model to Study the Adsorption Kinetics of Prednisolone on Six Carbonaceous Materials. *Journal of colloid and interface science, 248(1)*, 33-40.

[55] Pardo-Botello, R., Fernández-González, C., Pinilla-Gil, E., Cuerda-Correa, E. M., Gómez-Serrano, V. (2004). Adsorption kinetics of zinc in multicomponent ionic systems. *Journal of colloid and interface science*, *277*(2), 292-298.

[56] El-Naggar, M.R. and Metwally, S.S. (2011). Adsorption potential of Na-X zeolite in Sc-Sr-Co-multi-component system: kinetic and thermodynamic studies. *Isotope and radiation research, 43*(4), 1649-1665.